Nanoscale Advances

ROYAL SOCIETY OF CHEMISTRY

PAPER

View Article Online
View Journal | View Issue

Cite this: *Nanoscale Adv.*, 2025, **7**, 4425

A mussel-like, biodegradable natural hydrogel can effectively prevent adhesion after cardiac surgery†

Jie Jiang,[a] Liang Chen,[b] Yan Zhang[b] and Yan Liu *[b]

Postoperative cardiac tissue damage can lead to adhesions between the heart and surrounding tissues. These adhesions may result in restricted cardiac function, reduced quality of heart surgeries, and an increased risk of severe bleeding during reoperations. Therefore, it is essential to develop an effective anti-adhesion therapy to address postoperative cardiac adhesions. In this study, we propose a simple and easy-to-prepare adhesive hydrogel designed to prevent adhesions following cardiac surgery while maintaining normal cardiac pumping function. Dopamine was modified onto GelMA chains *via* a straightforward amidation reaction and mixed with silk fibroin to form a hydrogel (GelMA-DA/SF) under ultraviolet irradiation. *In vitro* experiments demonstrated that the GelMA-DA/SF hydrogel exhibited strong wet adhesion and could effectively degrade within 14 days. *In vivo* experiments showed that the GelMA-DA/SF hydrogel effectively prevented postoperative adhesions by reducing inflammation and friction. Therefore, the GelMA-DA/SF hydrogel is a reliable material for preventing postoperative adhesions and offers new insights and directions for subsequent therapeutic approaches.

Received 1st January 2025
Accepted 13th March 2025

DOI: 10.1039/d5na00005j

rsc.li/nanoscale-advances

1. Introduction

Pericardial adhesion refers to the adhesion formed between the heart, major blood vessels, and surrounding tissues.[1,2] It is also a major postoperative complication of cardiac surgery.[3,4] Tissue adhesion is essentially a self-defense response of the body, often causing symptoms such as pain, stiffness, and loss of function.[5,6] In cardiovascular surgery, particularly in cases of congenital heart disease, many patients require a second or even a third cardiac surgery.[7] After the first heart surgery, varying degrees of adhesion develop between the heart, major blood vessels, and surrounding tissues over time, significantly increasing the risk of fatal complications during subsequent surgeries.[8] Adhesions primarily occur due to inflammation and coagulation processes triggered by surgery, injury, or irritation. Initially, these adhesions manifest as inflammatory responses, which damage the monolayer of cells on the basement membrane in tissues.[9] A large amount of inflammatory cells and fibrin-rich serous material exudes, further leading to fibroblast attachment and the formation of the vascular system. These issues, along with a decrease in fibrinolytic activity, can result in the deposition of the extracellular matrix (ECM) and the formation of adhesions.[10] Currently, the primary approach to resolving postoperative adhesions is surgical adhesion lysis, but this method can lead to more severe recurrent adhesions.[11]

Recently, there has been a growing number of reports on anti-adhesion biomaterials.[12] These materials can effectively prevent postoperative adhesions by forming a physical barrier that isolates fibrin deposits from inflamed tissue surfaces.[13] However, several issues remain with their practical application. On one hand, anti-adhesion materials are difficult to completely degrade *in vivo*, potentially leading to postoperative infections and secondary injuries. On the other hand, common anti-adhesion materials have difficulty remaining at the wound site for extended periods, resulting in limited postoperative protection. Liu *et al.* designed a novel Janus hydrogel adhesive, where one side firmly adheres to gastric tissue, while the other side effectively prevents postoperative adhesions. Although this material exhibits good adhesive properties, the article did not report the duration of its adhesive effectiveness.[14] Guo *et al.* reported an underwater adhesive with anti-swelling properties that lasts for 7 days. However, the hydrogel contains various organic polymers, which not only increase the material's biotoxicity but also make it difficult to degrade, potentially causing secondary inflammation.[15] Therefore, we propose a biomaterial with wet adhesive properties that can effectively secure the heart and pericardium, reducing damage caused by postoperative friction.[16,17]

Injectable hydrogels are considered ideal materials for preventing postoperative adhesions.[18] On one hand, due to the injectability of hydrogel precursors, the liquid can be injected into the required site and form hydrogels under specific conditions, thereby increasing the contact area between the

[a]*Department of Cardiac Surgery, Zhongda Hospital, School of Medicine, Southeast University, Nanjing 210009, China*

[b]*Department of Cardiology, Nanjing First Hospital, Nanjing Medical University, Changle Road No. 68, Nanjing, Jiangsu 210006, China. E-mail: njyyly2024@163.com*

† Electronic supplementary information (ESI) available. See DOI: https://doi.org/10.1039/d5na00005j

material and the tissue.[19] On the other hand, hydrogels can serve as a barrier in the body to reduce friction between tissues. A variety of hydrogels derived from natural materials or synthetic polymers have been used to prevent postoperative adhesions.[20] Among various injectable hydrogels, UV-polymerizable hydrogels have received increasing attention for preventing postoperative adhesions due to their excellent operability. However, these hydrogels still face several challenges in biomedical applications, such as non-biodegradability, low mechanical strength, and rapid erosion at the injection site. Particularly, when used as anti-adhesive agents to prevent postoperative adhesions *in vivo*, common hydrogels tend to exhibit a short retention time. Therefore, developing new hydrogels with excellent biodegradability and biocompatibility for anti-adhesion applications remains a pressing need.[21]

Gelatin methacrylate (GelMA) has been widely used in biomedical engineering due to its excellent biocompatibility, controllable degradability, and photo-crosslinking properties.[22] On one hand, GelMA gels contain Arg-Gly-Asp (RGD) motifs and matrix metalloproteinases, which can provide sites for cell attachment. On the other hand, many studies have shown that catechol modification, inspired by mussels, can improve the poor adhesive properties of GelMA.[23,24] For example, it has been reported that catechol-modified GelMA adhesive nanosheets can effectively adhere to uneven tissue surfaces under wet conditions for extended periods.[25] Furthermore, various polymers, such as gelatin and silk fibroin, can form photo-crosslinked network structures by modifying photoactive groups and can be prepared as multifunctional wound dressings together with other hydrogels.[26] To date, developing photo-crosslinked hemostatic wound dressings with good adhesiveness, antibacterial properties, and hemostatic properties remains a major challenge.

As shown in Fig. 1, in this study, we developed a degradable, stable, adhesive, photopolymerizable hydrogel, GelMA-DA/SF. By characterizing the mechanical properties and adhesive strength of hydrogels with different compositions, we identified the most suitable hydrogel formulation, GelMA-DA/SF-2. Through *in vitro* and *in vivo* experiments, we demonstrated that the hydrogel we designed exhibits excellent biocompatibility, anti-inflammatory effects, and other functions. More importantly, the GelMA-DA/SF hydrogel reduces friction between the heart and pericardium, preventing the formation and worsening of cardiac adhesions following cardiac surgery.

2. Materials and methods

2.1 Reagents and cells

Gelatin methacrylate (GelMA), 1-ethyl-(3-dimethylaminopropyl) carbodiimide (EDC), *N*-hydroxysuccinimide (NHS), dopamine hydrochloride (DA), 2-hydroxy-4′-(2-hydroxyethoxy)-2-methylacetophenone (2959), and silk fibroin (avg. mol wt 100 kDa, SF) were purchased from Sigma. DMEM medium, DCFH-DA detection kit, live/dead staining (AM/PI) kit, and CCK-8 kit were obtained from Nanjing KeyGen Biotech Co., Ltd. Mouse fibroblast L929 cells were purchased from the Cell Research Institute of the Chinese Academy of Sciences.

2.2 Preparation of GelMA-DA/SF

2.2.1 Preparation of GelMA-DA. The synthetic route of GelMA-DA is shown in Fig. 2A. Pre-measured 1 g of GelMA was placed in a 50 mL conical flask with 9 mL of PBS and 9 mL of DMF, and stirred at 60 °C to completely dissolve the GelMA. Then, 1.5 g of EDC and 0.9 g of NHS were dissolved in 4 mL of DMF and added dropwise to the conical flask, followed by adjusting the pH of the system to 5 and stirring for 30 minutes. Then, 1 g of DA was dissolved in 1 mL PBS to prepare a 1 g per mL^{-1} DA solution, which was slowly added to the above solution and stirred in the dark at 60 °C for 10 hours. Subsequently, the solution in the conical flask was filtered through a 0.2 μm membrane to remove impurities. The filtrate was placed in a dialysis bag (8–14 kDa) and dialyzed in deionized water for 5 days to remove small molecular impurities. Finally, the dialyzed solution was stored at −80 °C for 12 hours, then freeze-dried to obtain foam-like GelMA-DA.

2.2.2 Preparation of the GelMA-DA/SF hydrogel. GelMA-DA, SF, and 2959 were mixed in different ratios as shown in Table 1, and exposed to UV light with an intensity of 50 mW and a wavelength of 345–385 nm for 5 minutes to form the hydrogel.

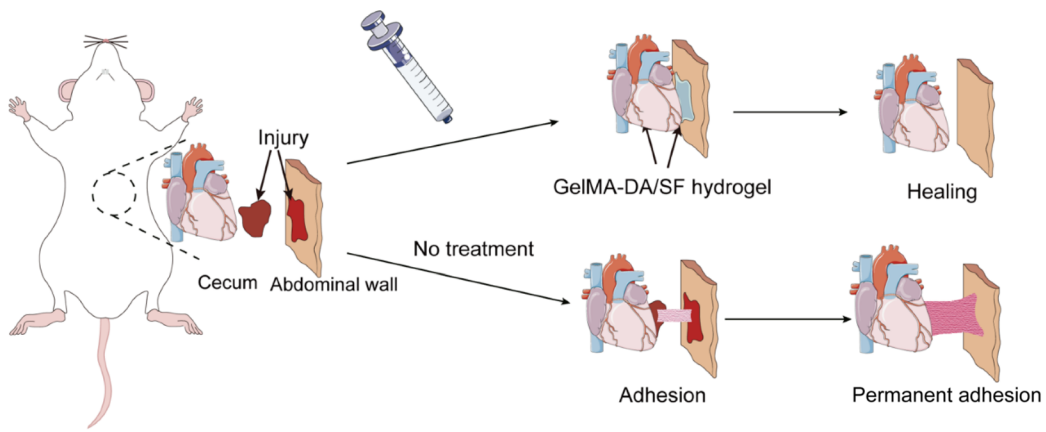

Fig. 1 Schematic illustration of the GelMA-DA/SF hydrogel preventing postoperative cardiac adhesions in rats.

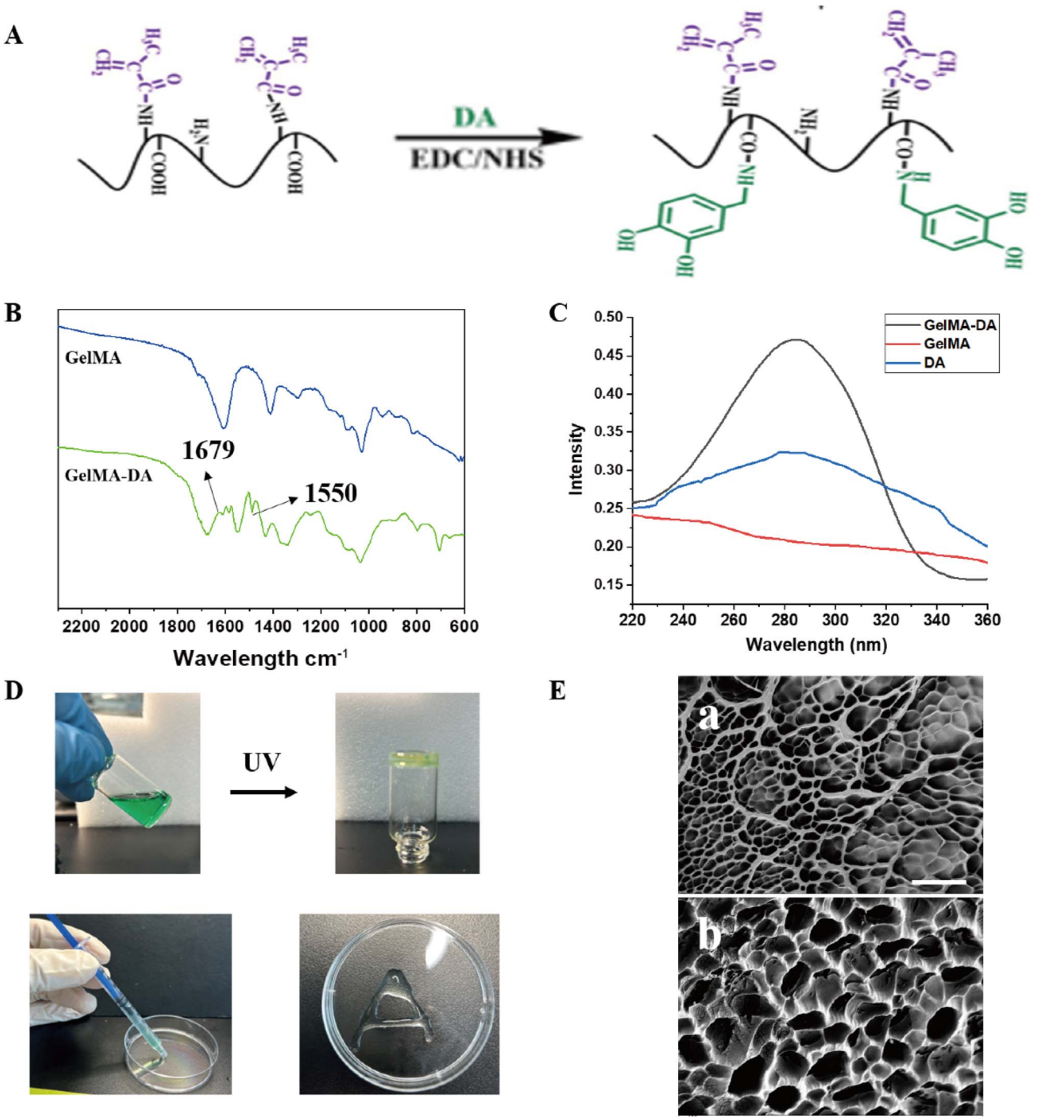

Fig. 2 Characterization of the GelMA-DA/SF hydrogel. (A) Schematic of GelMA-DA synthesis. (B) Infrared spectra of GelMA and GelMA-DA. (C) UV spectra of GelMA and GelMA-DA. (D) Demonstration of the GelMA-DA/SF hydrogel's rapid photopolymerization and injectability. (E) Typical scanning electron microscopy (SEM) image of (a) GelMA-DA/SF and (b) GelMA-DA hydrogels. Scale bar, 100 μm.

Table 1 GelMA-DA/SF Hydrogel Components

	GelMA-DA (w/w)	SF (w/w)	2959 (w/w)
GelMA-DA/SF-1	5	10%	1%
GelMA-DA/SF-2	5	20%	1%
GelMA-DA/SF-3	5	30%	1%

0.1 g of each hydrogel group was immersed in 10 mL of DMEM culture medium for 24 hours to obtain the hydrogel extract. The extract was then filtered using a 0.22 μm sterile filter and stored in 15 mL centrifuge tubes for future use.

2.3 Morphological characterization

The prepared hydrogel substrate was cut into 1.5 cm × 1.5 cm pieces and frozen at −20 °C. The pieces were then freeze-dried

and treated with liquid nitrogen. The samples were broken in half, with the cross-section facing upwards, fixed onto a scanning electron microscope (SEM, FEI Quanta S 4800) stage using conductive double-sided tape, and then sputter-coated with gold for observation.

2.4 Infrared spectroscopy

The prepared hydrogel substrate (200 mg) was frozen at −20 °C and then freeze-dried. The dried hydrogel was ground into a powder and pressed into a pellet under a 150 W infrared heat lamp, followed by analysis using an infrared spectrometer (PerkinElmer Spectrum 100 FTIR Spectrometer).

2.5 Swelling analysis

Swelling tests were conducted by immersing the dried hydrogel in deionized water. The hydrogel was weighed at regular intervals after wiping off surface water at room temperature. The swelling ratio (SR) was calculated using the formula:

$$\mathrm{SR} = \frac{W_1 - W_0}{W_0} \times 100$$

where W_0 is the sample weight before and W_1 is the weight after swelling, respectively.

2.6 Mechanical and adhesion performance testing

Rheological measurements were performed to assess the viscoelastic properties of the hydrogel using a rotational rheometer (MCR302, Anton Paar GmbH, Austria). The hydrogel sample (approximately 1 mL) was placed between the plates and the precursor solution exposed to UV light and subjected to oscillatory shear stress. The storage modulus (G') and loss modulus (G'') were recorded as a function of temperature or time. The gelation process was monitored by measuring the dynamic moduli under continuous oscillation at a frequency of 1 Hz. The temperature sweep was conducted over a range of 20 °C to 37 °C, and the gelation point was determined based on the crossover of G' and G''.

Then, take 10 μL of hydrogel precursor solution and apply it to the front end of a gelatin-coated glass slide. Then, overlap it with another gelatin-coated glass slide, ensuring the contact area between the two glass slides is the region coated with the hydrogel precursor solution. Place the overlapped glass slides under a UV lamp (50 mW and λ of 345–385 nm) for 5 minutes and immediately remove them afterward. Test the samples using a tensile testing machine (FLR-303, Flora Automation Technology). Fix the overlapped glass slides in the machine's clamps and set the tensile rate parameter to 1 mm min^{-1}. Measure the maximum load that the two glass slides can withstand before separating and calculate the adhesion strength of the hydrogel. Each sample group is tested in triplicate.

2.7 Cytotoxicity testing

Seed 5000 L929 cells in each well of a 96-well plate. Use complete DMEM (100 μL) for the control group, and culture the experimental group with the extract solution of hydrogel samples. After culturing the cells in the extract solution for 1, 3, and 5 days, wash the wells with PBS. Then, prepare a 10% CCK-8 working solution using the complete DMEM medium and CCK-8 reagent. Add 100 μL of the CCK-8 working solution to each well of the plate and incubate it at 37 °C in the dark for 2 hours. After incubation, place the plate on a shaker to mix thoroughly, and then use a Multiskan FC Microplate Reader (US Thermo) to measure the absorbance of each well at 450 nm.

Co-culture the hydrogel extract samples with 20 000 L929 cells in a 24-well plate. Use complete DMEM (100 μL) for the control group, while the experimental group is cultured with the extract solution of the hydrogel samples. After 24 hours of culture, wash the wells thoroughly with PBS to remove the medium. Then, treat the wells with a live/dead staining reagent by adding 200 μL of staining solution to each well and incubate for 30 minutes in a cell culture incubator. Finally, capture images and analyze them using a fluorescence microscope (Olympus BX53, Japan).

2.8 Real-time polymerase chain reaction (RT-PCR)

QRT-PCR was used to measure the gene expression levels. Total RNA was extracted from cells using TRIzol reagent (Invitrogen). RNA purity was checked using a NanoDrop 2000 spectrophotometer (Thermo Fisher Scientific, Waltham, MA, USA). RNA was reverse transcribed using the PrimeScript™ RT kit (Takara, Tokyo, Japan) and then the obtained cDNAs were quantified using RT-qPCR assay labelled with an SYBR Green PCR Mix Kit (Takara) according to the instructions. The RT-qPCR results were quantified with the 2-ΔΔCT method.

2.9 *In vivo* anti-adhesion testing

A cardiac adhesion model was used to test the *in vivo* anti-adhesion performance of the hydrogels.[27] Male SD rats (10–12 weeks) were obtained from Beijing Sibeifu Biotechnology Co., Ltd. SD rats were anesthetized with tribromoethanol, intubated, and mechanically ventilated. A thoracotomy was performed to expose the heart, and the pericardium was torn to expose it further. The exposed heart surface was punctured 100 times using a 30 mL needle and air-dried for 10 minutes. The experimental group injected 200 μL of GelMA-DA/SF hydrogel droplets onto the surface of the injured heart and irradiated it with 50 mW at a wavelength of 345–385 nm for 5 minutes to form the hydrogel, then closed the thoracic cavity and sutured the wound. In the control group, no treatment was applied before wound closure. After two weeks, the rats were dissected to observe the adhesion status. Tissue samples from the adhesion area, heart, lungs, spleen, liver, and kidneys were collected, paraffin-embedded, sectioned, and stained with H&E and Masson's trichrome. Images were obtained using a microscope (Olympus BX53, Japan) and Olympus imaging software.

2.10 Statistical analysis

Statistical significance in all graphs was indicated by P values (***, $P < 0.001$). Statistical differences were considered significant, and NS indicated no significant difference.

3. Results and discussion

3.1 Synthesis and characterization of GelMA-DA

GelMA-DA was synthesized using the method shown in Fig. 2A. Briefly, under the catalysis of EDC/NHS, the carboxyl groups on the GelMA chain were activated, allowing an amidation reaction with the amine groups on DA. The reaction product was characterized by infrared spectroscopy (Fig. 2B), where the characteristic peaks at 1550 cm^{-1} and 1679 cm^{-1} corresponded to the amide I and amide II bands, respectively. Additionally, ultraviolet (UV) spectroscopy was performed on the samples before and after DA grafting. As shown in Fig. 2C, DA exhibited a significant UV absorption peak at 280 nm, and the intensity of absorption increased with the DA concentration in the solution, due to the catechol groups on DA. These data confirm the successful synthesis of GelMA-DA. Subsequently, GelMA-DA was mixed with SF and polymerized under UV light to form a GelMA-DA/SF hydrogel (Fig. 2D). The hydrogel precursor displayed excellent injectability and rapid gelation, laying the foundation for subsequent *in vivo* experiments. SEM images showed that the GelMA-DA/SF hydrogel formed a three-dimensional network (Fig. 2E). When comparing the GelMA-DA/SF hydrogel with existing cardiac repair adhesives, our approach does not require complex synthesis steps, and the raw materials are all natural components with excellent biosafety. However, to improve the underwater adhesion strength of the material, we introduced catechol groups through chemical modification, which still somewhat limits the clinical application of the GelMA-DA/SF hydrogel. In future experiments, we hope to prepare porous or fibrous structures through electrospinning or freeze-drying to enhance underwater adhesion *via* mechanical interlocking. This still requires further validation. In summary, we grafted dopamine onto GelMA using EDC/NHS catalysis to form GelMA-DA. After confirming its structure through spectral characterization, we copolymerized it with SF to obtain a GelMA-DA/SF hydrogel with injectability, rapid gelation, and a three-dimensional network structure.

3.2 Mechanical properties and adhesion performance of GelMA-DA/SF hydrogels

To ensure that the GelMA-DA/SF hydrogel we designed can effectively prevent postoperative adhesions, it is necessary for the hydrogel to have sufficient wet adhesion strength to stabilize the heart's adhesion to the pericardium, reducing friction between the heart and surrounding tissues. Additionally, the GelMA-DA/SF hydrogel should be biodegradable post-surgery to minimize inflammation and wound complications caused by

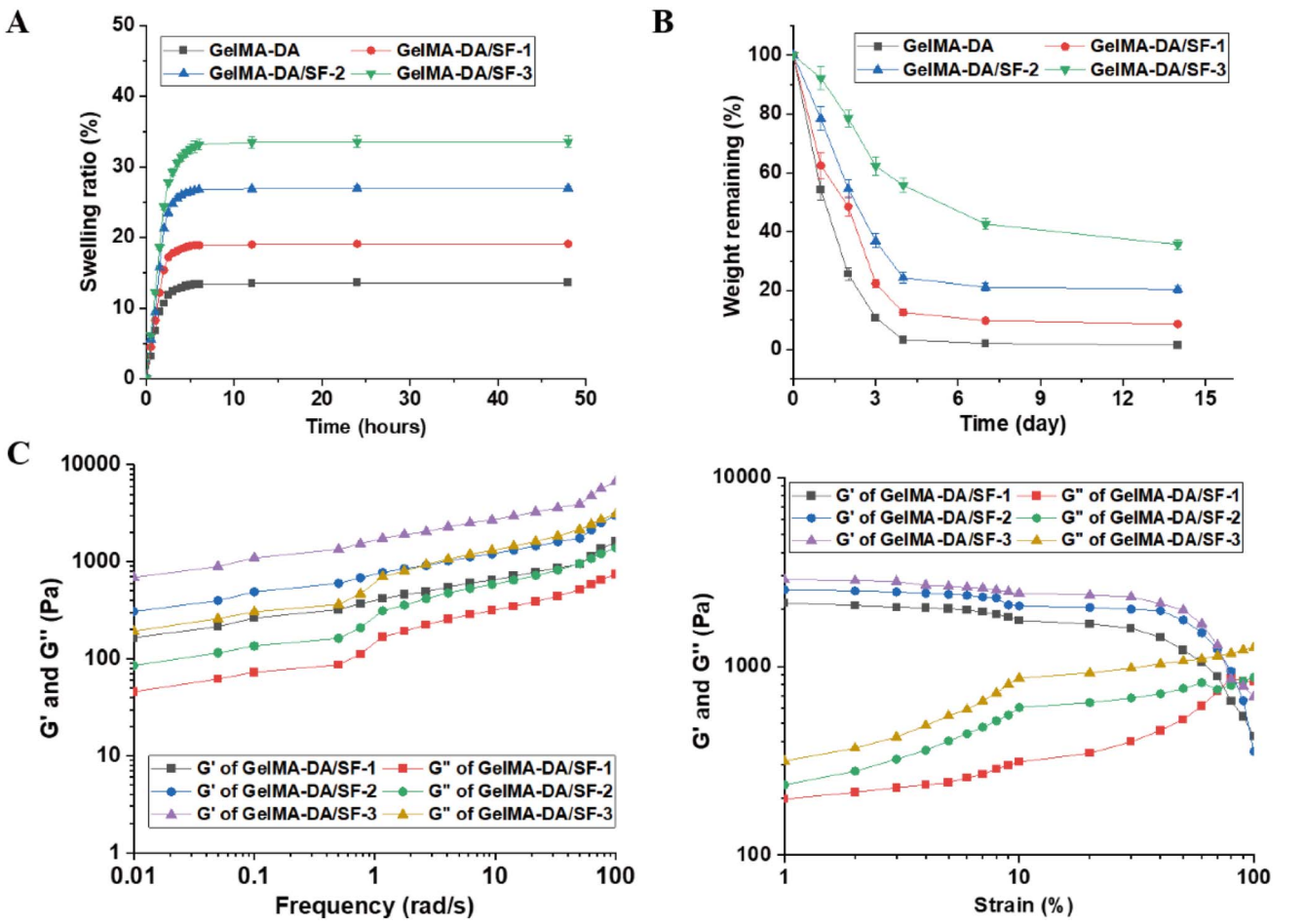

Fig. 3 Mechanical properties of the GelMA-DA/SF hydrogel. (A) Swelling curves and (B) degradation curves of hydrogels with different compositions. (C) Rheological properties of hydrogels with different compositions under two modes.

foreign materials. Therefore, we adjusted the SF content and labeled the hydrogels as GelMA-DA/SF-1, GelMA-DA/SF-2, and GelMA-DA/SF-3, and characterized their mechanical properties and adhesion strength.

As shown in Fig. 3A, the swelling ratio of the hydrogels increased over time, reaching equilibrium at around 8 hours. The swelling ratio also increased with higher SF concentrations. Furthermore, we analyzed the *in vitro* degradation performance of the hydrogels. As shown in Fig. 3B, the hydrogels gradually degraded over time, reaching equilibrium after approximately 3–4 days. The degradation rate of GelMA-DA/SF increased with higher SF concentrations, which is related to the degree of crosslinking within the hydrogel. Furthermore, we observed that after 14 days, more than 90% of the GelMA-DA/SF-1 group had degraded. This excellent degradability prevents secondary infections caused by foreign implants. Currently reported *in vivo* adhesives are often chemically synthesized gels, which, although they offer stable adhesion strength, still require surgical removal of the implant after treatment. In contrast, our polysaccharide-based hydrogel can degrade stably within 14 days, offering significant application value.

Rheological analysis further evaluated the mechanical properties of the hydrogels. As shown in Fig. 3C, within the range of 0.01–100 rad s^{-1}, the storage modulus (G') of the hydrogels was consistently greater than the loss modulus (G''), indicating the successful formation of GelMA-DA/SF hydrogels. The storage modulus of GelMA-DA/SF increased with higher SF concentrations, consistent with the degradation results. Under 1–100% strain, the hydrogels exhibited a crossover point between G' and G''. These data indicate that the designed hydrogels have good degradability, making them suitable for preventing *in vivo* adhesions.

The GelMA-DA/SF hydrogels also demonstrated excellent adhesion properties. As shown in Fig. 4A, the hydrogels adhered to various substrates and could attach wet rat viscera to glass slides. According to the procedure in Fig. 4B, we tested the adhesion strength of the hydrogels. As shown in Fig. 4C, the adhesion strength of pure GelMA-DA was only 1.4 kPa, which is related to the poor mechanical properties of GelMA hydrogels. After adding SF, the adhesion strength of GelMA-DA/SF significantly increased. As the SF concentration increased, the adhesion strength of GelMA-DA/SF hydrogels first increased and then decreased. This can be attributed to two factors. First, when the SF concentration is low, it may act as a reinforcing material, filling the structural gaps in GelMA to form a more compact network, thereby improving mechanical properties and adhesion strength. However, an excessive amount of SF

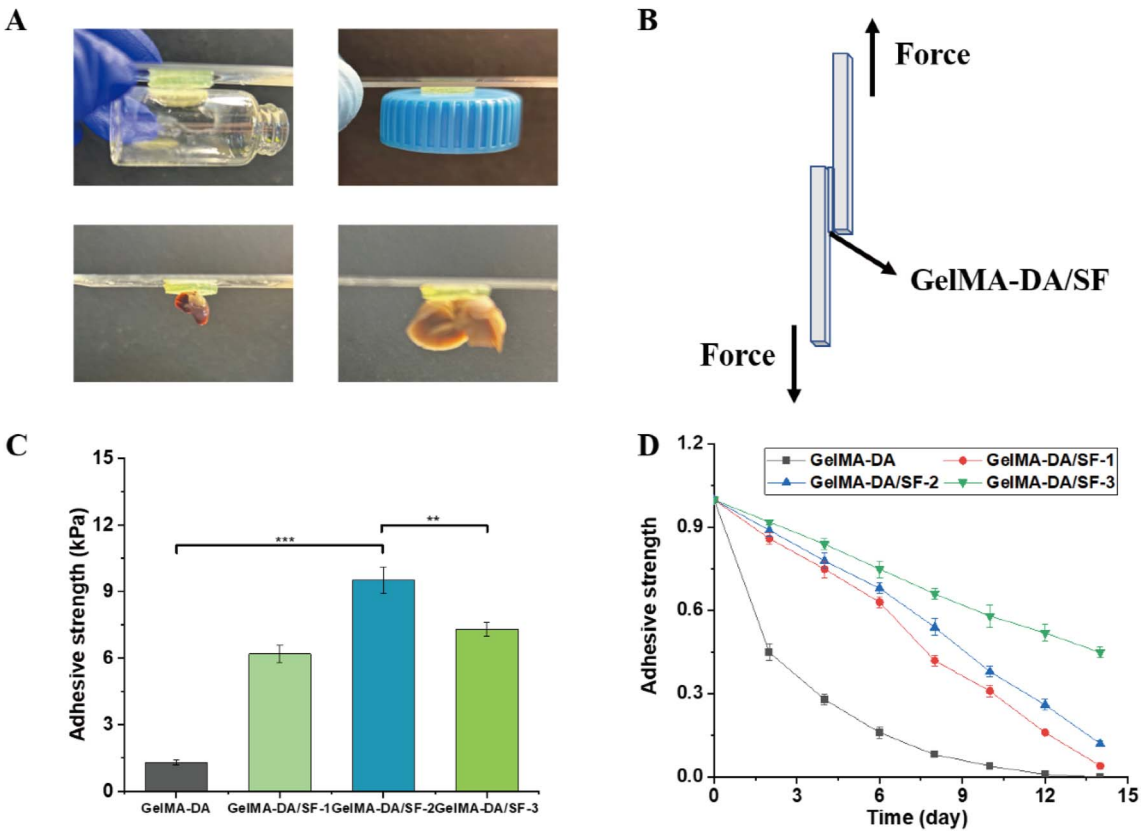

Fig. 4 Adhesion properties of the GelMA-DA/SF hydrogel. (A) GelMA-DA/SF hydrogel can adhere to various material surfaces (glass, plastic, *etc.*) and can also attach rat organs to glass. (B) Schematic diagram of the adhesion strength testing of the GelMA-DA/SF hydrogel. (C) Adhesion strength of the GelMA-DA/SF hydrogel with different compositions. (D) Adhesion strength of materials with different compositions over time. ($n \geq 3$), **, $p < 0.01$, ***$p < 0.001$.

may hinder the crosslinking of GelMA itself, forming an overly rigid structure that makes the hydrogel brittle and unable to effectively adhere to the surface, thus reducing adhesion strength. Additionally, SF can affect the swelling rate of the hydrogel. Appropriate swelling can promote interface wetting (such as filling surface micropores), but excessive swelling can lead to the accumulation of volumetric expansion stress, weakening the interfacial bonding. This results in our material exhibiting a trend of first increasing and then decreasing adhesion strength as the SF concentration increases. We also tested the stability of the adhesion strength of GelMA-DA/SF hydrogels. As shown in Fig. 4D, the adhesion strength of all hydrogel groups decreased over time, and the rate of decrease slowed with higher SF concentrations. On the 14th day, the adhesion strength of the GelMA-DA/SF-2 group was only 0.16 kPa. On one hand, the GelMA-DA/SF hydrogel provided adhesion prevention post-surgery, and on the other hand, it ensured post-surgical biodegradability. The GelMA-DA/SF-3 hydrogel maintained a high adhesion strength even after 14 days, which could hinder post-surgical heart recovery. Conversely, the GelMA-DA/SF-1 material exhibited poor mechanical properties. Therefore, we selected the GelMA-DA/SF-2 hydrogel for subsequent *in vivo* experiments.

3.3 Biocompatibility and anti-inflammatory properties

Good biocompatibility is essential for the success of *in vivo* experiments.[28] The cytotoxicity of GelMA-DA/SF-2 hydrogels was evaluated using live/dead staining and the CCK-8 assay. As shown in Fig. 5A, cells remained in good condition after 5 days of culture. The CCK-8 assay results also indicated that cell viability remained above 95% (Fig. 5B), demonstrating the excellent biocompatibility of our materials. Furthermore, our material also demonstrates excellent hemocompatibility (Fig. S1†). To test the *in vivo* biocompatibility of the PMPC polymer, we directly injected the GelMA-DA/SF-2 precursor solution into the peritoneal cavity and irradiated it with UV light for 10 minutes to form the hydrogel. After 14 days, we collected blood from the rats and performed hematological and clinical biochemical tests, as well as pathological evaluations of the organs. The hematological and clinical biochemical results were similar and showed no systemic toxicity (Tables 3 and 4). Moreover, we found no significant differences between the two groups in the HE staining (Fig. S3†), indicating that GelMA-DA/SF exhibits excellent *in vivo* biosafety.

Additionally, we tested the anti-inflammatory properties of GelMA-DA/SF-2 hydrogels. An inflammation model was established by co-culturing cells with LPS for 24 hours. Subsequently, GelMA-DA/SF hydrogel extracts were added, and ROS levels were measured after 24 hours. As shown in Fig. 5C and S2,† compared to the control group, the ROS levels in the GelMA-DA/SF group were significantly reduced. Furthermore, qt-PCR was used to detect the expression of inflammatory cytokines after GelMA-DA/SF-2 treatment. As shown in Fig. 5D, the expression of TNF-α, IL-6, and IL-8 was significantly reduced in the treatment group. These results indicate that GelMA-DA/SF-2 hydrogels not only have excellent biocompatibility but also possess strong anti-inflammatory effects *in vitro*, providing a basis for post-surgical recovery.

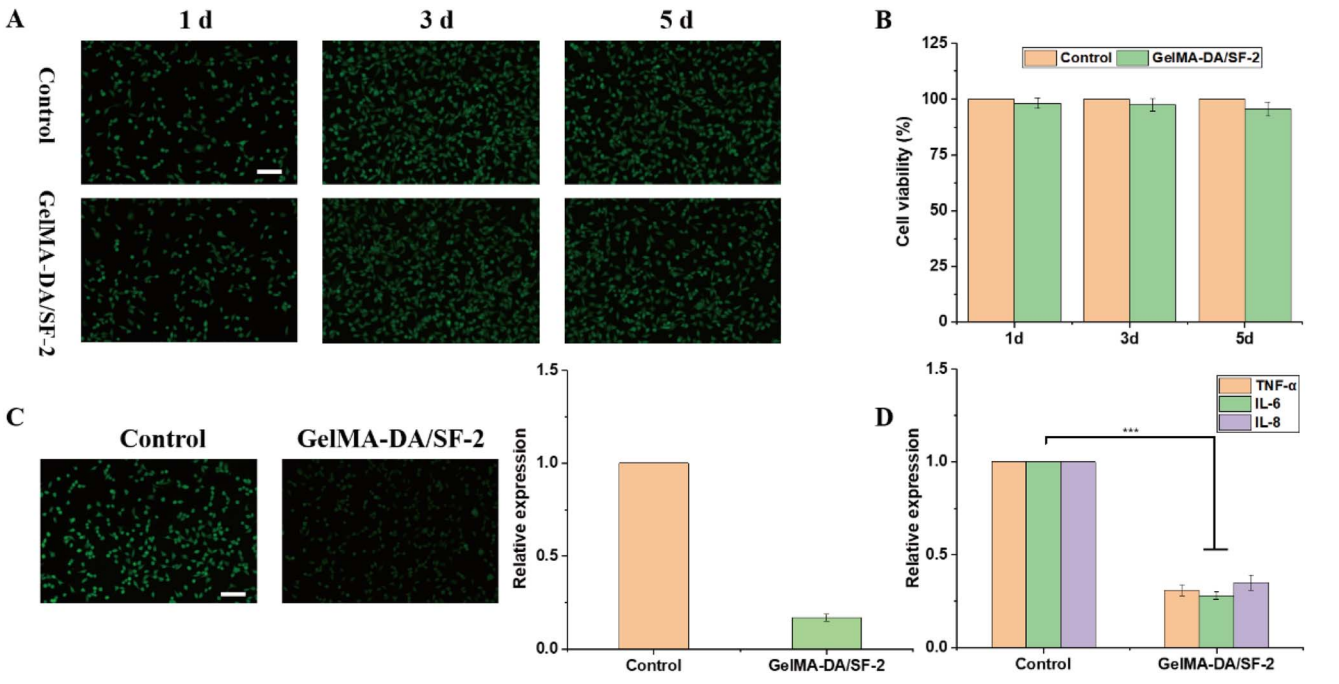

Fig. 5 *In vitro* biotoxicity of the GelMA-DA/SF hydrogel. (A) Live/dead staining images of L929 cells co-cultured with GelMA-DA/SF hydrogel extract for 1, 3, and 5 days (red: dead cells, green: live cells). (B) Quantitative analysis of cell density at 1, 3, and 5 days using CCK-8 assay. (C) Intracellular ROS detection in the LPS-induced inflammation group and GelMA-DA/SF hydrogel extract treatment group using DCFH-DA. (High fluorescence intensity indicates high intracellular ROS, and low fluorescence intensity indicates low intracellular ROS.) (D) Quantitative analysis of inflammation-related factors by qt-PCR. ($n \geq 3$), ***$p < 0.001$. Scale bar, 100 μm.

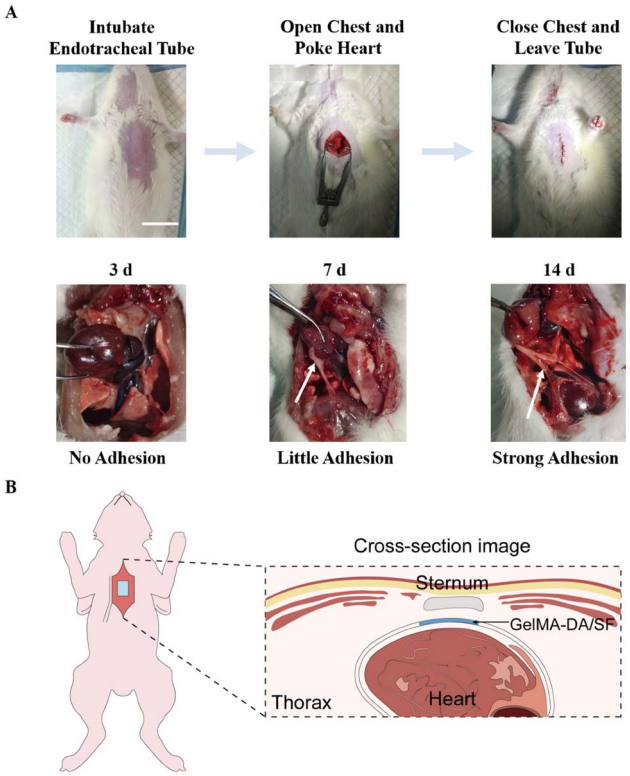

Fig. 6 Schematic and photographs of the rat heart adhesion model construction. (A) Heart images on post-operative day 3, day 7, and day 14. No heart adhesion is observed on day 3, slight adhesion between the heart and ribs on day 7, and strong adhesion on day 14. White arrows indicate the adhesion sites. Scale bar, 1 cm. (B) Schematic of the GelMA-DA/SF hydrogel's anti-adhesion effect *in vivo*.

Table 2 Peritoneal adhesion score grade for the *in vivo* adhesion test

Score	The condition of abdominal-blind cecum adhesion
0	No adhesions
1	Very little adhesion
2	Small to moderate amounts of adhesion
3	Moderate to substantial adhesion
4	Severe adhesion

Table 3 Chem summary of hematological data (mean ± SD)[a]

Parameters	GelMA-DA/SF-2	Control
WBC [10^9 L^{-1}]	8.62 ± 1.35	8.62 ± 1.53
RBC [10^{12} L^{-1}]	7.34 ± 1.35	7.22 ± 0.31
HgB [g L^{-1}]	146.67 ± 2.36	165.28 ± 4.73
PLT [10^9 L^{-1}]	658.25 ± 46.36	612.67 ± 42.34
NEUT [%]	18.17 ± 2.13	20.36 ± 3.42
LYMPH [%]	81.25 ± 4.22	75.44 ± 3.68
MONO [%]	4.74 ± 0.59	4.25 ± 0.64
EO [%]	0.37 ± 0.29	0.37 ± 0.06
BASO [%]	0.12 ± 0.02	0.11 ± 0.04
WBC [10^9/L]	9.25 ± 1.48	9.45 ± 1.23

[a] White blood cell (WBC); red blood cell (RBC); hemoglobin (HgB); platelet (PLT); neutrophil proportion (NEUT); lymphocyte proportion (LYMPH); monocyte proportion (MONO); eosinophil proportion (EO); basophil proportion (BASO).

3.4 The construction of the rat cardiac adhesion model

Based on previous studies, a rat cardiac adhesion model was selected to evaluate the anti-adhesion performance of GelMA-

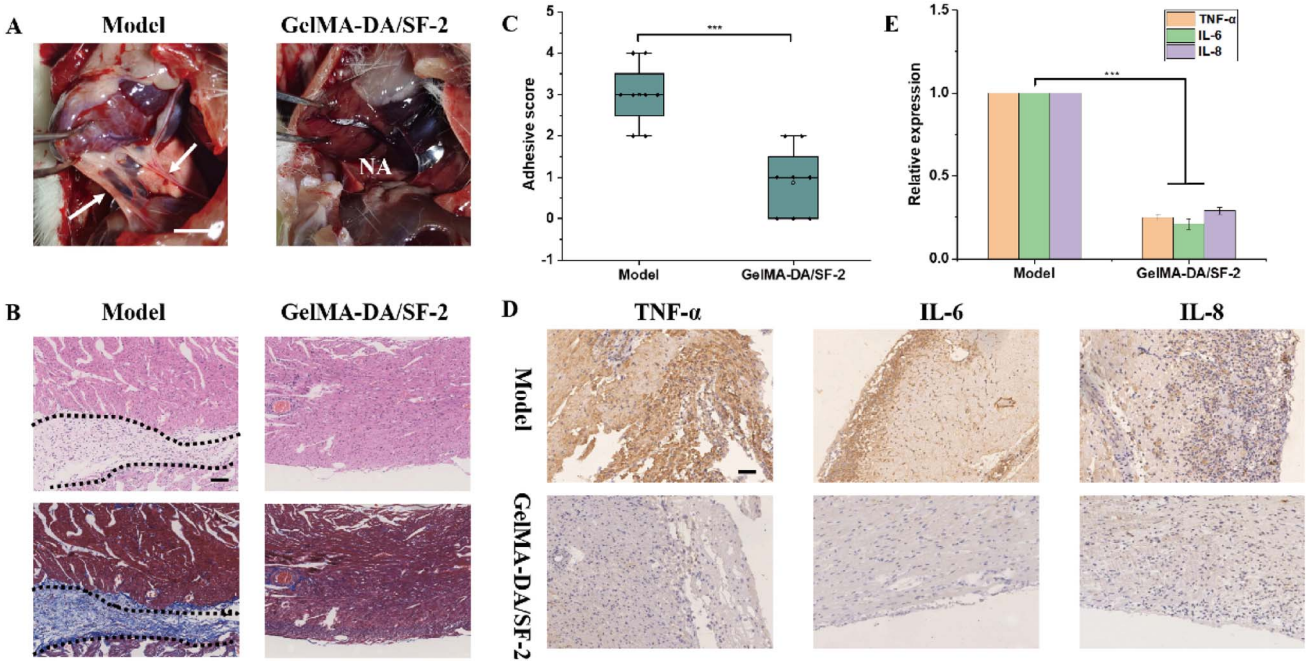

Fig. 7 Anti-adhesion effect of the GelMA-DA/SF hydrogel *in vivo*. (A) Photographs 14 days post-treatment, with white arrows indicating heart adhesions. Scale bar, 1 cm. (B) H&E staining and Masson staining of the model group and treatment group. The dashed areas represent adhesion tissues. (C) Adhesion score evaluation of the model group and GelMA-DA/SF treatment group 14 days post-treatment. (D) Immunohistochemical analysis of inflammation-related factors in the model group and GelMA-DA/SF treatment group. (E) Quantitative analysis of inflammation-related factors using qt-PCR in the model group and GelMA-DA/SF treatment group. ($n = 8$), ***, $p < 0.001$. Scale bar, 100 μm.

DA/SF-2 hydrogels. As shown in Fig. 6A, a schematic diagram illustrates the model. The procedure began with a midline neck incision to separate the thyroid. A left anterior chest incision was then made to separate the pectoralis major and serratus anterior muscles. The thoracic cavity was opened between the 4th and 5th ribs. To induce trauma, the heart surface was pricked 100 times and air-dried for 30 minutes. A drainage tube was placed before closing the thoracic cavity. After removing the tracheal tube, the tracheal and thoracic incisions were sutured.

As illustrated in Fig. 6B, the thoracic cavities were reopened on days 3, 7, and 14 to assess adhesion formation. No adhesion was observed on day 3, partial adhesion between the chest wall and heart was observed on day 7, and significant adhesion was seen by day 14. Thus, day 14 was selected as the sampling point for subsequent experiments. Injection of the GelMA-DA/SF-2 hydrogel into the pericardial space reduced friction between the heart and pericardium, thereby decreasing the likelihood of postoperative adhesions.

Table 4 Summary of clinical biochemistry data (mean ± SD)[a]

Parameters	GelMA-DA/SF-2	Control
ALT [U L^{-1}]	59.34 ± 4.65	62.33 ± 3.68
AST [U L^{-1}]	126.17 ± 8.52	131.58 ± 7.69
ALP [U L^{-1}]	94.68 ± 7.68	98.57 ± 7.35
BUN [mmol L^{-1}]	5.77 ± 0.44	6.74 ± 0.78
TP [g L^{-1}]	85.37 ± 4.17	93.03 ± 8.46
GLU [mmol L^{-1}]	0.59 ± 0.29	0.54 ± 0.06
CHOL [mmol L^{-1}]	2.36 ± 0.44	2.52 ± 0.24
TBIL [mmol L^{-1}]	1.20 ± 0.14	0.90 ± 0.16
CK-MB [U L^{-1}]	424.29 ± 36.58	384.29 ± 21.34
CR [μmol L^{-1}]	30.67 ± 2.52	30.42 ± 1.53

[a] Alanine amino transferase (ALT); aspartate amino transferase (AST); alkaline phosphatase (ALP); blood urea nitrogen (BUN); total protein (TP); glucose (GLU); cholesterol (CHOL); total bilirubin (TBIL); creatine kinase isoenzyme (CK-MB); creatinine (CR).

3.5 *In vivo* anti-adhesion performance

As shown in Fig. 7A, after 14 days of treatment, there was no adhesion tissue between the heart and chest walls of the GelMA-DA/SF-2 hydrogel group. However, the heart and chest walls of the model group were tightly adhered. Further histological analysis, including H&E and Masson staining, was conducted to evaluate tissue recovery in the treatment group. As illustrated in Fig. 7B, the results from the H&E and Masson staining corroborated the previous findings. In the staining images of the model group (as indicated by arrows), a significant amount of adhesion tissue was observed between the myocardium and ribs. The GelMA-DA/SF-2 hydrogel demonstrated a reduction in collagen deposition, which is likely a critical factor in preventing the formation of adhesions.

The adhesion scores of the two groups were evaluated using a scoring system that ranged from no adhesion to very dense vascularized adhesion.[29] Over 50% of the GelMA-DA/SF-2 hydrogel group scored 0, whereas the majority of the model group scored 4 or 5 (Fig. 7C and Table 2). Additionally, a pathological analysis of cardiac adhesion tissue was performed. As depicted in Fig. 7D and E, the treatment group showed a marked reduction in the expression of inflammation-related cytokines.

To further assess the impact of GelMA-DA/SF-2 hydrogels on rat organs, a pathological examination was carried out on the hearts, livers, spleens, lungs, and kidneys of both the SD rat

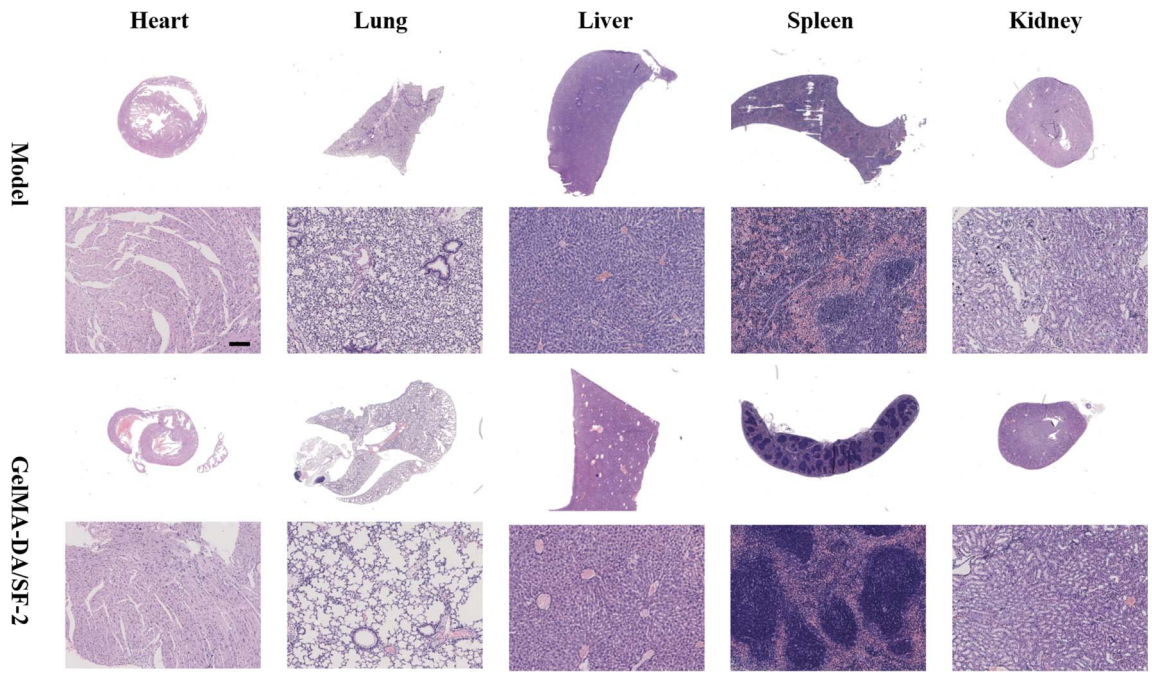

Fig. 8 *In vivo* biosafety of the GelMA-DA/SF hydrogel. H&E staining images of the heart, lungs, liver, spleen, and kidneys of rats 14 days post-surgery in the model group and GelMA-DA/SF group. Scale bar, 100 μm.

model group and the GelMA-DA/SF-2 hydrogel group. As shown in Fig. 8A, in comparison to the treatment group, the model group exhibited more void-like structures between myocardial fibers in the left ventricular tissues, likely due to adhesion-induced cardiac dysfunction. Rats in the model group also demonstrated extensive inflammatory cell infiltration and significant pulmonary congestion in the lungs. Furthermore, varying levels of hepatic, splenic, and renal congestion were noted in all rats, indicating right ventricular dysfunction, which was more pronounced in the model group. In contrast, the GelMA-DA/SF-2 hydrogel group showed only mild cardiac dysfunction, characterized by splenic and renal congestion, which is likely attributed to direct cardiac injury during model establishment rather than cardiac adhesion. Overall, the GelMA-DA/SF-2 hydrogel effectively prevented cardiac adhesions and helped maintain the normal function of other organs in the rats.

4. Conclusion

In this study, we developed a simple and easily prepared adhesive hydrogel for the prevention of post-cardiac surgery adhesions. The ratio of components in the GelMA-DA/SF hydrogel was optimized through rheological analysis and adhesion performance testing, and the selected GelMA-DA/SF-2 hydrogel was used for subsequent experiments. The *in vitro* results showed that the GelMA-DA/SF hydrogel exhibited excellent wet adhesion properties, could adhere to various substrates, and degraded by 80% within 14 days. Additionally, the GelMA-DA/SF hydrogel demonstrated good biocompatibility and anti-inflammatory effects. *In vivo* experiments indicated that the GelMA-DA/SF hydrogel could prevent cardiac adhesions by reducing inflammation and minimizing friction between the heart and pericardium. Therefore, the GelMA-DA/SF hydrogel we designed is a safe and effective approach, providing new insights and methods for preventing postoperative adhesions in cardiac surgery patients.

Ethical statement

All animal procedures were performed in accordance with the Guidelines for Care and Use of Laboratory Animals of Nanjing Medical University and experiments were approved by the Animal Ethics Committee of Nanjing First Hospital.

Data availability

The data are available in the main manuscript, ESI† files, and from the corresponding authors upon reasonable request.

Author contributions

J. J. contributed to the experimental design and data analysis, L. C. and Y. Z. were responsible for the synthesis and characterization of the biodegradable natural hydrogel, and Y. L. supervised the project and provided guidance throughout the research process. All the authors reviewed the manuscript.

Conflicts of interest

The authors declare that they have no competing interests.

References

1 S. J. Wu, J. Wu, S. J. Kaser, H. Roh, R. D. Shiferaw, H. Yuk, *et al.*, A 3D printable tissue adhesive, *Nat. Commun.*, 2024, **15**(1), 1215.
2 P. Chansoria, A. Chaudhari, E. L. Etter, E. E. Bonacquisti, M. K. Heavey, J. Le, *et al.*, Instantly adhesive and ultra-elastic patches for dynamic organ and wound repair, *Nat. Commun.*, 2024, **15**(1), 4720.
3 Y. Wang, W. Zhai, H. Zhang, S. Cheng and J. Li, Injectable Polyzwitterionic Lubricant for Complete Prevention of Cardiac Adhesion, *Macromol. Biosci.*, 2023, **23**(4), e2200554.
4 L. M. Stapleton, A. N. Steele, H. Wang, H. Lopez Hernandez, A. C. Yu, M. J. Paulsen, *et al.*, Use of a supramolecular polymeric hydrogel as an effective post-operative pericardial adhesion barrier, *Nat. Biomed. Eng.*, 2019, **3**(8), 611–620.
5 J. Stehlik, J. Kobashigawa, S. A. Hunt, H. Reichenspurner and J. K. Kirklin, Honoring 50 Years of Clinical Heart Transplantation in Circulation, *Circulation*, 2018, **137**(1), 71–87.
6 H. E. Emam and T. I. Shaheen, Design of a dual pH and temperature responsive hydrogel based on esterified cellulose nanocrystals for potential drug release, *Carbohydr. Polym.*, 2022, **278**, 118925.
7 S. Li, W. Ahmed, S. Wang, X. Hu, B. Wang, Z. Wang, *et al.*, Bi-layered polyurethane nanofiber patches with asymmetrical surface prevent postoperative adhesion and enhance cardiac repair, *Composites, Part B*, 2024, **283**, 111668.
8 E. Zhang, J. Li, Y. Zhou, P. Che, B. Ren, Z. Qin, *et al.*, Biodegradable and injectable thermoreversible xyloglucan based hydrogel for prevention of postoperative adhesion, *Acta Biomater.*, 2017, **55**, 420–433.
9 H. Fan, J. Wang and J. P. Gong, Barnacle Cement Proteins-Inspired Tough Hydrogels with Robust, Long-Lasting, and Repeatable Underwater Adhesion, *Adv. Funct. Mater.*, 2020, **31**(11), 2009334.
10 Y. Lv, F. Cai, X. Zhao, X. Zhu, F. Wei, Y. Zheng, *et al.*, Bioinspired Microstructured Janus Bioadhesive for the Prevention of Abdominal and Intrauterine Adhesions, *Adv. Funct. Mater.*, 2024, **34**(21), 2314402.
11 T. Wu and W. Liu, Functional hydrogels for the treatment of myocardial infarction, *NPG Asia Mater.*, 2022, **14**(9), 1–15.
12 D. Zhu, Z. Li, K. Huang, T. G. Caranasos, J. S. Rossi and K. Cheng, Minimally invasive delivery of therapeutic agents by hydrogel injection into the pericardial cavity for cardiac repair, *Nat. Commun.*, 2021, **12**(1), 1412.
13 M. Fujita, G. M. Policastro, A. Burdick, H. T. Lam, J. L. Ungerleider, R. L. Braden, *et al.*, Preventing post-surgical cardiac adhesions with a catechol-functionalized oxime hydrogel, *Nat. Commun.*, 2021, **12**(1), 3764.
14 C. Cui, T. Wu, X. Chen, Y. Liu, Y. Li, Z. Xu, *et al.*, A Janus Hydrogel Wet Adhesive for Internal Tissue Repair and

Anti-Postoperative Adhesion, *Adv. Funct. Mater.*, 2020, **30**(49), 2005689.

15 Y. Liang, H. Xu, Q. Han, M. Xu, J. Zhang, J. Wang, *et al.*, A Janus hydrogel sealant with instant wet adhesion and anti-swelling behavior for gastric perforation repair, *Nano Today*, 2024, **54**, 102105.

16 G. M. Taboada, K. Yang, M. J. N. Pereira, S. S. Liu, Y. Hu, J. M. Karp, *et al.*, Overcoming the translational barriers of tissue adhesives, *Nat. Rev. Mater.*, 2020, **5**(4), 310–329.

17 S. Huang, D. Lei, Q. Yang, Y. Yang, C. Jiang, H. Shi, *et al.*, A perfusable, multifunctional epicardial device improves cardiac function and tissue repair, *Nat. Med.*, 2021, **27**(3), 480–490.

18 Y. Liu, Q. Wang, X. Liu, P. Nakielski, F. Pierini, X. Li, *et al.*, Highly Adhesive, Stretchable and Breathable Gelatin Methacryloyl-based Nanofibrous Hydrogels for Wound Dressings, *ACS Appl. Bio Mater.*, 2022, **5**(3), 1047–1056.

19 M. Montgomery, S. Ahadian, L. Davenport Huyer, M. Lo Rito, R. A. Civitarese, R. D. Vanderlaan, *et al.*, Flexible shape-memory scaffold for minimally invasive delivery of functional tissues, *Nat. Mater.*, 2017, **16**(10), 1038–1046.

20 L. Song, L. Li, T. He, N. Wang, S. Yang, X. Yang, *et al.*, Peritoneal adhesion prevention with a biodegradable and injectable N,O-carboxymethyl chitosan-aldehyde hyaluronic acid hydrogel in a rat repeated-injury model, *Sci. Rep.*, 2016, **6**(1), 37600.

21 C. K. Roy, H. L. Guo, T. L. Sun, A. B. Ihsan, T. Kurokawa, M. Takahata, *et al.*, Self-Adjustable Adhesion of Polyampholyte Hydrogels, *Adv. Mater.*, 2015, **27**(45), 7344–7348.

22 P. Rao, T. L. Sun, L. Chen, R. Takahashi, G. Shinohara, H. Guo, *et al.*, Tough Hydrogels with Fast, Strong, and Reversible Underwater Adhesion Based on a Multiscale Design, *Adv. Mater.*, 2018, **30**(32), e1801884.

23 A. Hasan, A. Khattab, M. A. Islam, K. A. Hweij, J. Zeitouny, R. Waters, *et al.*, Injectable Hydrogels for Cardiac Tissue Repair after Myocardial Infarction, *Adv. Sci.*, 2015, **2**(11), 1500122.

24 Z. Zhang, J. Ni, L. Chen, L. Yu, J. Xu and J. Ding, Encapsulation of cell-adhesive RGD peptides into a polymeric physical hydrogel to prevent postoperative tissue adhesion, *J. Biomed. Mater. Res., Part B*, 2012, **100**(6), 1599–1609.

25 J. Yu, K. Wang, C. Fan, X. Zhao, J. Gao, W. Jing, *et al.*, An Ultrasoft Self-Fused Supramolecular Polymer Hydrogel for Completely Preventing Postoperative Tissue Adhesion, *Adv. Mater.*, 2021, **33**(16), e2008395.

26 Y. He, Q. Li, P. Chen, Q. Duan, J. Zhan, X. Cai, *et al.*, A smart adhesive Janus hydrogel for non-invasive cardiac repair and tissue adhesion prevention, *Nat. Commun.*, 2022, **13**(1), 7666.

27 M. Cencer, Y. Liu, A. Winter, M. Murley, H. Meng and B. P. Lee, Effect of pH on the Rate of Curing and Bioadhesive Properties of Dopamine Functionalized Poly(ethylene glycol) Hydrogels, *Biomacromolecules*, 2014, **15**(8), 2861–2869.

28 L. Yuan, H. Wei, Z. Pan, X. Deng, L. Yang, Y. Wang, *et al.*, A bioinspired injectable antioxidant hydrogel for prevention of postoperative adhesion, *J. Mater. Chem. B*, 2024, **12**(28), 6968–6980.

29 X. Wang, L. Xiang, Y. Peng, *et al.*, Gelatin/Polycaprolactone Electrospun Nanofibrous Membranes: The Effect of Composition and Physicochemical Properties on Postoperative Cardiac Adhesion, *Front. Bioeng. Biotechnol.*, 2022, **10**, 862276; *Front. Bioeng. Biotechnol.*, 2021, **9**, 792893.